



The Thermal Conductivity of Near-Eutectic Galinstan ($\text{Ga}_{68.4}\text{In}_{21.5}\text{Sn}_{10}$) Molten Alloy

Maria José V. Lourenço¹ · Miguel Alves¹ · João M. Serra² · Carlos A. Nieto de Castro¹ · Matthias H. Buschmann³

Received: 3 November 2023 / Accepted: 8 November 2023 / Published online: 13 December 2023
© The Author(s) 2023

Abstract

The need for new heat transfer agent for many applications, namely in the consumer electronics industry, requires materials, liquids at room temperature, with high thermal conductivity. From the different possibilities, Galinstan, a eutectic alloy of Gallium, Indium, and Tin with a melting point ($T_m = 283.4$ K) has been proposed for many applications, namely for replacing the toxic mercury element, used for many years. It is the purpose of this paper to report thermal conductivity measurements of Galinstan, product name Gallium/Indium/Tin Eutectic (NL-011), $\text{Ga}_{68.4}\text{In}_{21.5}\text{Sn}_{10}$. The method used was the transient hot strip (THS), using a platinum metal-film sensor, produced by PVD in ceramic substrates, and electrically insulated with a heat-shrinkable coating. The details of the data acquisition system and measuring procedure are reported. Measurements were performed between 28 °C and 103 °C (301 K to 376 K), at atmospheric pressure, with an estimated uncertainty of 6%,

Selected Papers of the 22nd European Conference on Thermophysical Properties.

✉ Carlos A. Nieto de Castro
cacastro@ciencias.ulisboa.pt

Maria José V. Lourenço
mjlourenco@ciencias.ulisboa.pt

Miguel Alves
miguelasalves97@gmail.com

João M. Serra
jmserra@ciencias.ulisboa.pt

Matthias H. Buschmann
Matthias.Buschmann@ilkdresden.de

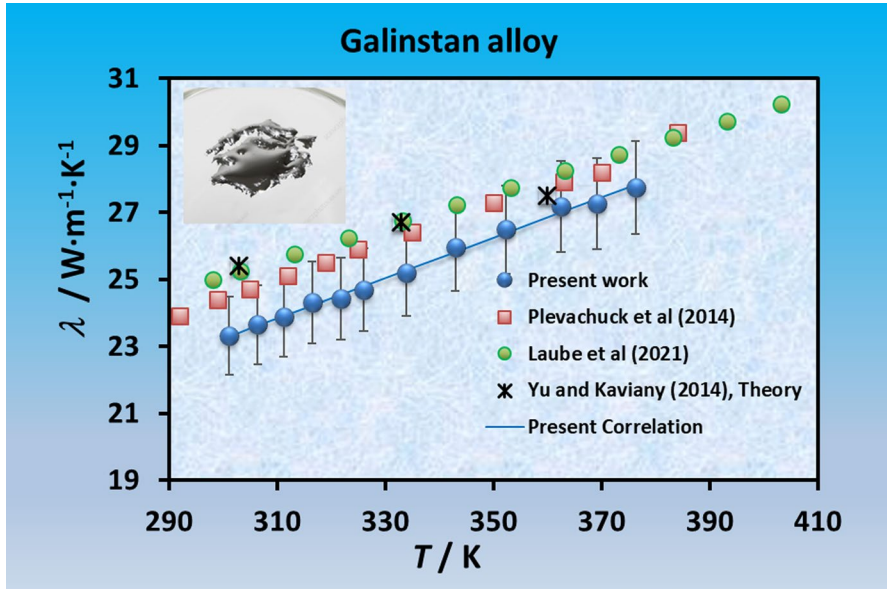
¹ Centro de Química Estrutural, Institute of Molecular Sciences, Departamento de Química e Bioquímica, Faculdade de Ciências, Universidade de Lisboa, Campo Grande, 1749-016 Lisbon, Portugal

² Instituto D. Luís, Faculdade de Ciências, Universidade de Lisboa, Campo Grande, 1749-016 Lisbon, Portugal

³ Institut Für Luft- Und Kältetechnik gGmbH Dresden, 01309 Dresden, Germany

and compared with available literature. Data were correlated for linear interpolation. This type of sensor is applied to molten metals for the first time, proofing to concept to future applications in molten metals and molten salts at higher temperatures.

Graphical Abstract



Keywords Galinstan · Molten eutectic alloy · Thermal conductivity · Transient hot strip

1 Introduction

The need for new heat transfer agent for many applications, namely in the consumer electronics industry, requires electrical conducting materials, liquid at room temperature, with high thermal conductivity [1, 2]. In addition, the prohibition to use liquid mercury in many applications, namely in some thermometers and electronic switches, due to the toxic parameters and their danger to human health [3], led to the search of convenient metals to replace it. From the different possibilities, Galinstan, a eutectic alloy of gallium, indium, and tin with a melting point ($T_m=283.4$ K) [2] has been proposed for many applications, namely for replacing mercury, a toxic element used for many years [3, 4].

Within the methods that can be used to measure the thermal conductivity ionic melts, including electrically conducting liquids, at high temperatures, conveniently described in a recent publication [5], the transient methods have been found to achieve, if applied according to the best knowledge of their mathematical descriptions, to be considered as primary methods. As approved by the CCQM—Comité

Consultatif pour la Quantité de Matière, BIPM, in 1995—a primary method of measurement is a method having the highest metrological qualities, the operation of which can be completely described and understood, for which a complete uncertainty statement can be written down in terms of SI units, the results of which are, therefore, accepted without reference to a standard of the quantity being measured [6]. From these, the transient hot wire, is capable of attaining and expanded uncertainty smaller than 1%, if a careful application of method is done, and an optimal design of the instrument is performed [7, 8].

As one of the most promising and robust methods for high-temperature applications, the transient hot strip, is potentially a primary method, if the 3D heat transfer equation is solved for the geometries involved (a metal thin film deposited in a ceramic substrate), which is not the case yet. Efforts to develop instrumentation capable are an important step to achieve a primary method status. In our laboratory, and following the developments already presented to use the transient hot strip method to determine the thermal conductivity of gaseous mixtures up to 800 °C [9], we are currently developing an instrument to measure molten metals and high-temperature molten salts, namely molten carbonates for concentrated solar power stations. This paper shows the “proof of concept” for these new applications, by constructing a sensor to measure the thermal conductivity of molten Galinstan, a conductive and corrosive alloy, from room temperature up to 103 °C, the temperature interval of the major part of the application of this alloy, prone to surface oxidation at higher temperatures.

2 Materials and Methods

2.1 Material

Galinstan was produced by Haines & Maassen Metallhandelsgesellschaft mbH, Bonn, Germany, with product name Gallium/Indium/Tin Eutectic (NL-011) and received from ILK, Dresden, in PE bottles (liquid), with a stated density of 6440 kg·m⁻³. The composition of the eutectic alloy was given by the manufacturer, as Ga_{68.4}In_{21.5}Sn₁₀, although there is the presence of some components like Cu and Pb (around 0.0035 wt%) and Al and Zn (<0.00005 wt%). The total composition is presented in Table 1.

The samples were handled with care, following the recommendations present in MSDS, as they are corrosive and irritant.

2.2 Method

The theory of the transient-hot strip was developed by Gustafsson and co-workers [9, 10] for an infinitely long and infinitely thin strip. Assuming that the “end effects” are non-existing, the main solution for the temperature rise in the hot strip ΔT_s can be approximated by Eq. 1:

Table 1 Composition of Ga_{68.4}In_{21.5}Sn₁₀ eutectic alloy, in mass %

Element	Mass fraction (%)
Ga	68.4 ± 0.684
In	21.5 ± 0.215
Sn	10.0 ± 0.100
Al	< 5 × 10 ⁻⁵
Pb	3.5 × 10 ⁻³ ± 3.5 × 10 ⁻⁴
Cu	1 × 10 ⁻³ ± 1 × 10 ⁻⁴
Zn	< 5 × 10 ⁻⁵

$$\tau = \frac{2\sqrt{k_f t}}{w} k_f = \frac{\lambda}{\rho C_p}, \quad (1)$$

$$\Delta T_s = T(t) - T_0 = \frac{q_s}{2\lambda\sqrt{\pi}} f(\tau),$$

$$f(\tau) = \tau \operatorname{erf}\left(\frac{1}{\tau}\right) - \frac{\tau^2}{\sqrt{4\pi}} \left[1 - \exp\left(-\frac{1}{\tau^2}\right)\right] + \frac{1}{\sqrt{4\pi}} E_1\left(\frac{1}{\tau^2}\right),$$

where k_f is the thermal diffusivity of the media, q_s is the heat dissipated per unit length of the strip, w is the width of the strip, τ is a dimensionless time, and λ , ρ , and C_p are, respectively, the thermal conductivity, density, and heat capacity of the fluid media. The mathematical functions $\operatorname{erf}(y)$ and $E_1(z)$ are, respectively, the error function and the exponential integral, obtainable from rational approximations and easily programmed [11]. From Eq. 1, the ratio $\Delta T/f(\tau)$ is inversely proportional to the thermal conductivity and directly proportional to the heat dissipation per unit length, and therefore, it will be possible to use this solution as the base of the application of this model to calculate the thermal conductivity of the fluid. In the paper by Queirós *et al.* [8] we have shown that, for arbitrary values of $0 < \tau < 465$, the function $f(\tau)$ can be translated as Eq. 2, a fact that simplifies data processing:

$$f(\tau) = 0.56417847 \ln(\tau) + 0.6835194. \quad (2)$$

The thermal conductivity of the ideal hot strip, immersed in a fluid media, can then be obtained from Eq. 3:

$$\Delta T_s = \frac{q_s}{2\lambda\sqrt{\pi}} [0.56417847 \ln(\tau) + 0.6835194] = a \ln(\tau) + b, \quad (3)$$

$$\lambda = \frac{q_s}{2\sqrt{\pi}} \frac{0.56417847}{a},$$

with $a = 0.56417847$ and $b = 0.6835194$.

The real model that will describe the sensor, needs several modifications, as the strip is not infinitely long or infinitely thin, neither it is floating in space, and has finite properties; therefore, it can store heat while being warmed. In addition, the platinum metal film has to be electrically insulated from electrically conducting media.

However, if

- i) the time length is adequately chosen to be greater than the time, then strip needs to be warmed (heat wave reaches the media), as explained before [8] and,
- ii) two strips differing only in the length are used to compensate for the end effects, these factors can be minimized. Therefore, in our equipment, a long and a short strip are used, and the “strip difference” properties are measured.
- iii) a ceramic sheet supports the strips, and an insulating coating has to be built. Therefore, and following Gustafsson development of the theory [12], the measured thermal conductivity is an effective property, λ_{eff} given by Eq. 4:

$$\lambda_{\text{eff}} = (\lambda_{\text{fluid}} \times \lambda_{\text{ceramic}})^{1/2}, \quad (4)$$

where λ_{ceramic} is the thermal conductivity of the ceramic support.

Having obtained the slope a of the temperature rise of the strip difference of our sensor as a function of τ (or t), we can obtain the estimated thermal conductivity. The reference temperature of the measurements was calculated assuming that it was equal to that of a measurement with a transient hot wire [4], as explained below.

3 Measuring Instrument

3.1 The Sensor

Inspired in the procedure developed many years ago to minimize the “end effects,” when in the real system we have a finite length strip, ceramic/thin metal-film-based sensors with two strips were constructed as described before [13, 14] and detailed for the current sensor [7], with physical dimensions given by hot strip length, $l_L = 15$ mm, short strip $l_S = 5$ mm, strip width $w = 110$ μm , and thickness $t = 0.34$ μm . Details of the construction process were described elsewhere and will not be repeated here [8, 13, 14].

The main obstacle was the coating development. First, we have used a sensor coated with a thin film of ceramic, deposited by PVD, as previously reported. However, we arrived to the conclusion that, after some years due to aging factors and manufacturers modifications, this coating was porous to water and Galinstan, breaking the electrical insulation and impeding measurements. This solution was very elegant but did not work. Several other products, like alumina pastes, alumina sprays, and alumina paints did not work also. As a final solution, we tried to use a halogen-free, flexible, flame retardant heat-shrinkable tubing, KTG-CB-HFT25.4, made by CYG (Changyuan Electronics, Dongguan Co., Ltd., China), supporting 125 °C, which could fit the sensor as a sleeve, and with good radial and longitudinal

Fig. 1 The thermal conductivity sensor after heat-shrinkable tubing application. Gray shadows were caused by Galinstan melt wetting. Ruler in cm and inches



shrinking properties. The material details are not disclosed by the company, just irradiated cross-linked modified polyolefin. On shrinking the tube, we tried to avoid bubbles staying inside the sensor.

Figure 1 shows the sensor used, after the measurements with Galinstan.

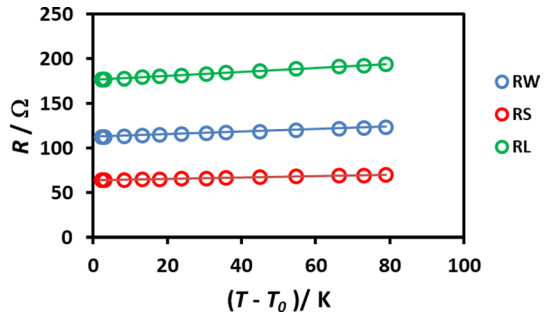
The instrument was completed by vertical tubular furnace, with temperature control (EUROTHERM 91e) up to 0.2 K, a ceramic crucible (Alumina), a platinum resistance thermometer (ASL, WIKA, GTH 7000), calibrated, with a standard uncertainty of 0.01 °C, and a supporting structure.

3.2 The Data Acquisition System

The data acquisition system was fully described in [8]. The sensor is part of a Wheatstone bridge circuit, which compensates for the end effects, a differential amplifier and Picolog 1612 unit (a 16 Channel Data logger of PICO TECHNOLOGY), equipped with a USB interface.

The resistances of the long strip (R_L) and short strip (R_S) were calibrated as a function of temperature in a temperature calibration facility in CIENCIAS ULISBOA Laboratory between room temperature and 373 K. The results were found to have a linear dependence on temperature, exemplified for the resistance of the strip length difference, $R_W = R_L - R_S$, given by Eq. 5:

Fig. 2 Strip resistances (R_L , R_S , and R_W) variation with temperature



$$R_W(T) = R_W(T_0) [1 + \alpha_{RW}(T - T_0)], \tag{5}$$

where α_{RW} , the mean coefficient of variation of the resistance with the temperature, was found to be 0.001270 ± 0.000001 . In this equation, $T_0 = 293.15$ K. The values for the individual strips were found to be, respectively, $\alpha_{RL} = 0.001263 \pm 0.00009$, $\alpha_{RS} = 0.001251 \pm 0.00003$, the ratio of the resistances being independent of temperature. These agreements make us believe that both strips have very similar electrical properties, and the success of the “end-effect” compensation can be assured. Figure 2 shows the resistances of the strips and the “ideal” floating strip (the strip length difference), as a function of temperature.

The transient resistance variation and temperature rise in the Transient Hot Strip (THS) sensor can be calculated from the bridge configuration, as described in [8], and given by Eq. 6:

$$R_W(t) = R_W(0) [1 + \alpha_{RW} \Delta T_W],$$

$$\Delta T_W = \frac{\Delta R_W(t)}{\alpha_{RW} R_W(0)}. \tag{6}$$

Keeping in mind that for $t=0$, the temperature of the strip is assumed to be in equilibrium at the fluid temperature, T_b . In addition, using two strips, a short and long one, with lengths l_S and l_L , the heat dissipated in the strip, per unit length, q_w can be evaluated from the applied voltage, for a strip of length $l_W = l_L - l_S$, by Eq. 7:

$$q_w = \frac{V^2 R_w}{(R_L + R_S + R_3)^2} \frac{1}{(l_L - l_S)}, \tag{7}$$

where V is the applied voltage and $R_3 = 270 \Omega$.

As explained in the previous application, the ideal model for the hot strip given by Eq. 3, has to be demonstrated to occur for the real application, and in the complex geometry of our system, only when the heat wave dissipated in the strips reaches the coating/fluid interface. Figure 3 shows one run (T28) with Galinstan, at $T_b = 348.01$ K, the linear part of the full run in the inset, and from which the

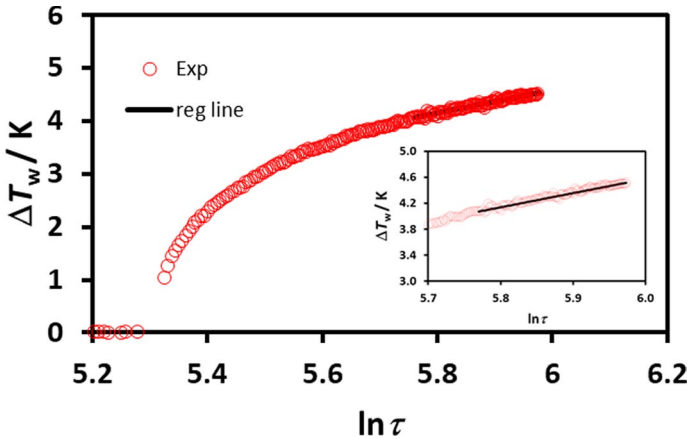


Fig. 3 The experimental transient temperature rises in the “strip difference,” ΔT_w , as a function of $\ln \tau$, for a run with Galinstan at $T_b = 348.01$ K. The inset shows the detail of the regression line, in the linear operational region

thermal conductivity was calculated. Deviations of the experimental points in the linear region to the fit do not amount to more than $\pm 1.5\%$, as shown in Fig. 4.

4 Results and Discussion

To obtain the thermal conductivity, we need to estimate the effect of the coating and ceramic support in the transient heat transfer in the sensor. The coating is made from a heat-shrinkable tubing, as explained above, which has an estimated thermal

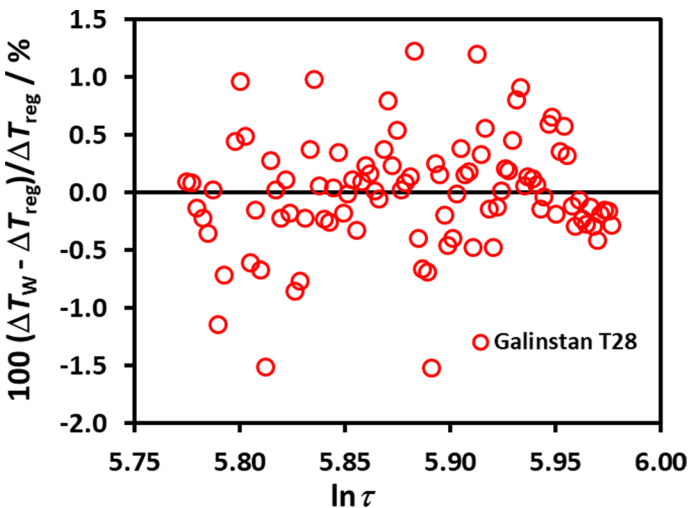


Fig. 4 Percentages deviations of the experimental temperature rise from the linear regression (the ideal model), as a function of $\ln \tau$

conductivity of $0.19 \text{ W}\cdot\text{m}^{-1}\cdot\text{K}^{-1}$ to $0.25 \text{ W}\cdot\text{m}^{-1}\cdot\text{K}^{-1}$ (manufacturers data, before shrinking).

No data exist for the shrank tube. The ceramic support, made from Rubalit 708S CeramTec, Marktredwitz, Germany), for which the value of the thermal conductivity, between 296 K and 1000 K, was measured by NETZSCH, Selb, Germany, and the values can be found in Lourenço PhD thesis (1998) [15] and used in references [8, 13, 14]. The value varies between $25.5 \text{ W}\cdot\text{m}^{-1}\cdot\text{K}^{-1}$ at 296 K and $22.3 \text{ W}\cdot\text{m}^{-1}\cdot\text{K}^{-1}$ at 373 K, about 100 times greater than the estimated value for the heat-shrinkable tube. Therefore, the thermal resistance of the ceramic support (about the same thickness of the tube coating) is 100 times smaller than the that of this coating, which will control the rate of heat transfer, the thermal resistance (and therefore, the thermal conductivity) of the system ceramic+thin platinum film+coating can be assumed to be that of the heat-shrinkable tubing (considering the resistance of the platinum film also negligible) and consequently

$$R_{\text{sensor}} = R_{\text{coating}} + R_{\text{film}} + R_{\text{ceramic}} \sim R_{\text{coating}}, \quad (8)$$

and Eq. 4 can be used, replacing λ_{ceramic} by λ_{coating} .

In order to validate this hypothesis, we have made measurements of the thermal conductivity of water, within the range of the present measurements, to estimate the thermal conductivity of the shrank tube. The value of the thermal conductivity of water was obtained from the standard reference data of IUPAC, published by Ramires et al. [16]. In Fig. 5, we show the validation test for water at 297 K, from which we obtained a value of $\lambda_{\text{coating}} = 0.175 \text{ W}\cdot\text{m}^{-1}\cdot\text{K}^{-1}$. Other tests with water at higher temperatures (up to 70 °C) showed no temperature dependence, so an average value of $0.18 \pm 0.01 \text{ W}\cdot\text{m}^{-1}\cdot\text{K}^{-1}$ was assumed (a standard uncertainty of 0.022, in relative terms). The calculation of the uncertainty of the measurements was made using ISO_GUM guidelines, expressing the contributions of all variables in the measurement, due to the sensor geometry (length, width), resistance calibration, voltage, and time measurement in the data acquisition system. These contributions to the standard uncertainty amounted to 0.015. Using a propagation factor $k=2$, we obtain $U_r(\lambda) = 2 \times (0.022^2 + 0.015^2) = 0.053$. Consequently, the estimated expanded relative uncertainty at a 95% confidence level ($k=2$), $U_r(\lambda) = 0.06$, was assumed for the experimental thermal conductivity data of Galinstan.

The results obtained for the thermal conductivity of Galinstan ($\text{Ga}_{68.4}\text{In}_{21.5}\text{Sn}_{10}$) are presented in Table 2.

The experimental data show a linear dependence on temperature in this temperature interval, given by Eq. 9:

$$\frac{\lambda}{\text{W}\cdot\text{m}^{-1}\cdot\text{K}^{-1}} = a_0 + a_1 \left(\frac{T}{\text{K}} \right). \quad (9)$$

In this equation, $a_0 = (21.61485 \pm 0.090160) \text{ W}\cdot\text{m}^{-1}\cdot\text{K}^{-1}$, $a_1 = (6.0182 \pm 0.13561) \times 10^{-2} \text{ W}\cdot\text{m}^{-1}\cdot\text{K}^{-2}$ and a root-mean-square deviation of $0.12 \text{ W}\cdot\text{m}^{-1}\cdot\text{K}^{-1}$. Deviations of the experimental points from the regression line are never bigger than 0.46%, as shown in Fig. 6, consistent with the estimated uncertainty of the reported data.

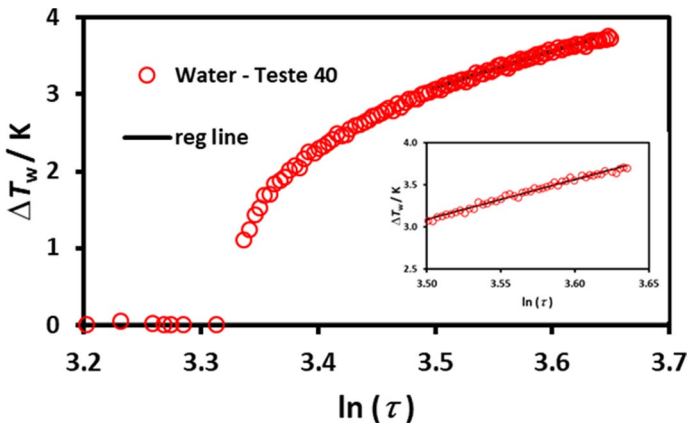


Fig. 5 A typical run for the validation of the experimental method with water, at 297 K, where the transient hot strip model is verified

The thermal conductivity of Galinstan has been measured by several workers. However, the composition is not always the eutectic composition, but “quasi” eutectic, and this might explain some of the differences found. In Table 3, we show the available data in the literature, identifying the alloy composition, the method of measurement, temperature interval, and estimated uncertainty, for available data.

In Fig. 7, we show all the available data, plotted for the temperature range 290 K to 410 K. It is clear that the data of Prohkorenko *et al.* [17–19] is far apart from the other sets of data, including the theoretical calculations, using the Bridgman model (for the molecular liquid thermal conductivity) and the Wiedemann–Franz law and the metal Lorentz number), for the electronic component [21]. This fact was already noticed by Plevachuck *et al.* [1], stating that these discrepancy (also observed at higher temperatures), citing “Experimental difficulties related to convection, uncertain wetting conditions, an insufficient level of purity, or oxidation effects can significantly reduce the accuracy of thermal conductivity measurements. Indeed, the aforementioned problems could be responsible for such a large variance between different data sets.”

The other three sets of data agree within their mutual uncertainty, our data being slightly smaller than Plevachuck *et al.* [1] and Laube *et al.* [19], but having almost identical temperature coefficients. The small difference in the alloy composition might explain these differences, as our alloy is poorer in tin and richer in gallium.

Finally, we would like to say that we cannot assure that no air was kept inside the shrank sleeve. Air bubbles can represent an additional heat transfer resistance/loss that might decrease the temperature rise in the strips. This can be systematic, and therefore, does not contribute to the slope and can be neglected, or depending on temperature rise/time, and affect the thermal conductivity reported, possibly explaining the smaller value measured for the thermal conductivity of Galinstan. Attempts to diminish this effect would be done in a near future.

Table 2 Thermal conductivity (uncertainty (95% confidence level), $U_r(\lambda) = 0.06$), λ_{exp} , of Galinstan ($\text{Ga}_{68.4}\text{In}_{21.5}\text{Sn}_{10}$) as a function of temperature

T ($^{\circ}\text{C}$)	T (K)	λ_{exp} ($\text{W}\cdot\text{m}^{-1}\cdot\text{K}^{-1}$)	T_{nom} (K)	λ_{nom} ($\text{W}\cdot\text{m}^{-1}\cdot\text{K}^{-1}$)
28.01	301.16	23.33	300	23.23
33.25	306.40	23.64	305	23.53
38.07	311.22	23.89	310	23.83
43.31	316.46	24.31	315	24.13
48.64	321.79	24.41	320	24.43
52.84	325.99	24.69	325	24.74
60.77	333.92	25.18	330	25.04
69.79	342.94	25.95	335	25.34
79.15	352.30	26.48	340	25.64
89.37	362.52	27.18	345	25.94
96.00	369.15	27.27	350	26.24
103.13	376.28	27.74	355	26.54
			360	26.84
			375	27.74
			370	27.44
			375	27.74

Values of the thermal conductivity at nominal temperatures, λ_{nom} , are also presented

Fig. 6 Deviations, in %, of the experimental points from Eq. 9. Dashed lines represent the root-mean-square deviation of the fit (0.46%)

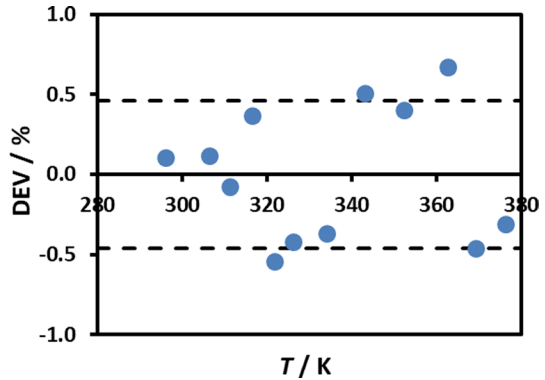


Table 3 Available data for the thermal conductivity of Galinstan

Authors	Method of measurement	T (K)	Mass composition	Estimated uncertainty	References
Prokhorenko et al. (1970, 1982, 2000)	Relative steady state axial flow method	368–673	$\text{Ga}_{67}\text{In}_{20.5}\text{Sn}_{12}$	6% (error)	[17–19]
Plevachuck et al. (2014)	Steady-state concentric cylinder	291–723	$\text{Ga}_{67}\text{In}_{20.5}\text{Sn}_{12.5}$	7% 10% at low temperature	[1]
Laube et al. (2021)	Laser flash apparatus	298–403	$\text{Ga}_{65.9}\text{In}_{20.3}\text{Sn}_{13.8}$	4.2%	[20]
Yu et al. (2014)	Theory	303–360	$\text{Ga}_{77.2}\text{In}_{14.4}\text{Sn}_{8.4}$	NA, Model	[21]
Present work	Transient hot strip	301–376	$\text{Ga}_{68.4}\text{In}_{21.5}\text{Sn}_{10}$	6%	

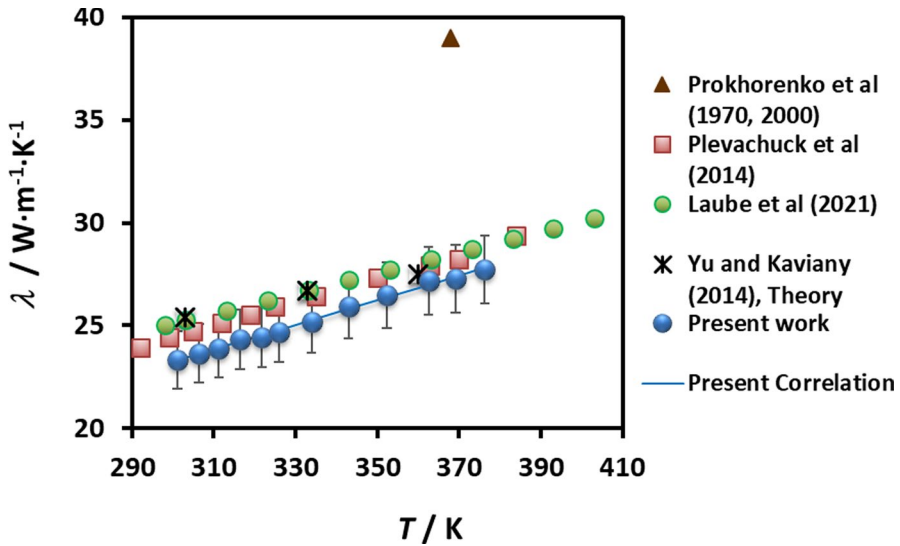


Fig. 7 The thermal conductivity of Galinstan. Present data and literature data, including theoretical calculations (Bridgmann model and Wiedmann–Franz law) [21]. The error bars in our data display our estimated uncertainty (6%)

5 Conclusions

New data on the thermal conductivity of molten Galinstan have been presented, by using the transient hot strip (THS) method. The sensors now developed, can be improved in the future, namely by using a different coating material, in order to extend the temperature range of the measurements. The measuring bridge is also under revision to improve signal to noise ratio. The theory of the method is approximate, and there are still improvements, at an analytical method, by developing a 3D model heat transfer model for the system. Application to measure the thermal conductivity of gallium and molten carbonate salt mixtures is under study.

Acknowledgements This work was supported by Fundação para a Ciência e Tecnologia, Portugal, through Projects UID/QUI/00100/2013, UID/QUI/00100/2019, and UIDB/00100/2020 and UIDP/00100/2020, by Institute of Molecular Sciences, an Associate Laboratory funded by FCT through Project LA/P/0056/2020 and by the Bundesministerium für Wirtschaft und Klimaschutz der Bundesrepublik Deutschland under Research Grant 49MF200081. A previous version of the sensors was financed by Gas-Pro-Bio Waste Project (FP7-SME-2010-1-261911), granted to University of Lisbon.

Author Contributions MB and MA prepared the samples. MJVL and JMS developed and constructed the automatic bridge and the sensors. MA, MJVL, and CANC made the measurements. MB and MJVL participated in the guidance of Galinstan properties and revision of the paper. CANC wrote the manuscript and supervised the work. All authors revised the manuscript.

Funding Open access funding provided by FCTIFCCN (b-on).

Declarations

Conflict of interest The authors declare no competing interests.

Open Access This article is licensed under a Creative Commons Attribution 4.0 International License, which permits use, sharing, adaptation, distribution and reproduction in any medium or format, as long as you give appropriate credit to the original author(s) and the source, provide a link to the Creative Commons licence, and indicate if changes were made. The images or other third party material in this article are included in the article's Creative Commons licence, unless indicated otherwise in a credit line to the material. If material is not included in the article's Creative Commons licence and your intended use is not permitted by statutory regulation or exceeds the permitted use, you will need to obtain permission directly from the copyright holder. To view a copy of this licence, visit <http://creativecommons.org/licenses/by/4.0/>.

References

1. Y Plevachuk V Sklyarchuk S Eckert G Gerbeth R Novakovic 2014 J. Chem. Eng. Data 59 757
2. P Maivald S Sridar W Xiong 2022 Thermo 2 1
3. Commission Delegated Regulation (EU) 2023/2049 of 14 July 2023 Amending Regulation (EU) 2017/852 of the European Parliament and of the Council as Regards Mercury-Added Products Subject to Manufacturing, Import and Export Prohibitions
4. S Handschuh-Wang FJ Stadler X Zhou 2021 J. Phys. Chem. CChem. C 125 20113
5. CA Nieto de Castro MJV Lourenço 2020 Energies 13 99
6. VMB Nunes MJV Lourenço FJV Santos MLS Matos Lopes CA Nieto de Castro 2010 Chapter 17, accurate measurement of physico-chemical properties on ionic liquids and molten salts KE Seddon M Gaune-Escard Eds Ionic Liquids and Molten Salts: Never the Twain Wiley New York
7. MJ Assael KD Antoniadis D Velliadou WA Wakeham 2023 Int. J. Thermophys. 44 85
8. CSGP Queirós MJV Lourenço SI Vieira JM Serra CA Nieto de Castro 2016 Rev. Sci. Instrum. 87 065105
9. SE Gustafsson E Karawacki MN Khan 1979 J. Phys. D 12 1411
10. SE Gustafsson E Karawacki MN Khan 1981 J. Appl. Phys. 52 2596
11. AM Abramowitz IA Stegun 1972 Handbook of Mathematical Functions 8 Dover Publications Inc New York
12. SE Gustafsson 1987 Rigaku J. 4 16
13. MJV Lourenço JM Serra MR Nunes AM Vallêra CA Nieto de Castro 1998 Int. J. Thermophys. 19 1253
14. MJV Lourenço JM Serra MR Nunes CA Nieto de Castro 1997 Integrated thin films and applications Ceram. Trans. 86 213
15. M.J.V. Lourenço, PhD Thesis, University of Lisbon (1998)
16. MLV Ramires CA Nieto de Castro Y Nagasaka A Nagashima MJ Assael WA Wakeham 1995 J. Phys. Chem. Ref. Data 24 1377 1381
17. V.Ya. Prokhorenko, E.A. Ratushnyak, B.I. Stadnyk, V.I. Lakh, A.M. Koval, Teplofiz. Vys. Temp. 8(2), 374–378 (1970); High Temp. 8(2), 346–350 (1970)
18. VY Prokhorenko VV Roshchupkin MA Pokrasin SV Prokhorenko VV Kotov 2000 High Temp. 38 954 968
19. V.Ya. Prokhorenko, The structure and electric properties of binary metal alloys. In *Obzory po teplofizicheskim svoistvam veshchestv; IVTAN*, vol. 6 (Institute of High Temperatures, USSR Academy of Sciences, Moscow, 1982), pp. 3–88
20. T. Laube, F. Emmendorfer, B. Dietrich, L. Marocco, Luca, T. Wetzel, *Thermophysical Properties of the Near Eutectic Liquid Ga–In–Sn Alloy*, Internal Report No. 1000140052 (Karlsruher Institute of Technology, 2021). <https://publikationen.bibliothek.kit.edu/1000140052>
21. S Yu M Kaviany 2014 J. Chem. Phys. 140 064303

Publisher's Note Springer Nature remains neutral with regard to jurisdictional claims in published maps and institutional affiliations.